Highly stable ultrabroadband mid-IR optical parametric chirped-pulse amplifier optimized for superfluorescence suppression

J. Moses,^{1,*} S.-W. Huang,¹ K.-H. Hong,¹ O. D. Mücke,¹ E. L. Falcão-Filho,¹ A. Benedick,¹ F. Ö. Ilday,¹ A. Dergachev,² J. A. Bolger,³ B. J. Eggleton,³ and F. X. Kärtner¹

¹Department of Electrical Engineering and Computer Science and Research Laboratory of Electronics,

Massachusetts Institute of Technology, Cambridge, Massachusetts 02139, USA

²Q-Peak, Incorporated, Bedford, Massachusetts 01730, USA

³Centre for Ultrahigh Bandwidth Devices for Optical Systems, Australian Research Council Centre of Excellence,

School of Physics, University of Sydney, Sydney, NSW 2006, Australia

*Corresponding author: j moses@mit.edu

Received February 2, 2009; revised April 1, 2009; accepted April 14, 2009; posted April 29, 2009 (Doc. ID 106923); published May 21, 2009

We present a 9 GW peak power, three-cycle, 2.2 μm optical parametric chirped-pulse amplification source with 1.5% rms energy and 150 mrad carrier envelope phase fluctuations. These characteristics, in addition to excellent beam, wavefront, and pulse quality, make the source suitable for long-wavelength-driven high-harmonic generation. High stability is achieved by careful optimization of superfluorescence suppression, enabling energy scaling. © 2009 Optical Society of America OCIS codes: 320.7110, 190.4970, 230.4480, 270.2500.

Since the prediction of high-yield, soft-x-ray (>120 eV photon energy) high-harmonic generation (HHG) in gases with mid-IR drive pulses [1–6], the development of low-noise, high-energy, few-cycle, carrier-envelope-phase (CEP) stable light pulse sources in this wavelength range has attracted wide Ultrabroadband optical chirped-pulse amplification (OPCPA) is a competitive route toward this technology—it is, to date, unique in its demonstrated ability to produce few-cycle pulses with multiterawatt peak power, achieved at 800 nm wavelength [7,8]. Recent work has extended fewcycle OPCPA to 2 µm wavelength with multigigawatt peak powers; intrapulse difference-frequency generation (DFG) of a 5 fs Ti:sapphire (Ti:S) oscillator output provides half-octave-bandwidth self-CEPstabilized 2 µm wavelength seed pulses, and Ndbased amplifiers seeded by the same oscillator produce high-energy picosecond pump pulses at 1 μ m for degenerate parametric amplification at 2 μ m with half-octave phase-matching bandwidth in bulk periodically poled lithium niobate [9,10]. Scaling of these systems to both higher pulse energy and average power for use as an HHG drive laser (e.g., using >100 W cryogenically cooled Yb:YAG 1 µm wavelength picosecond lasers [11] as the OPCPA pump) seems promising as a route to high-flux, tabletop, soft-x-ray HHG sources.

Extension of the OPCPA technology to the fewcycle, high-energy regime, however, has uncovered difficulty in achieving satisfying noise performance, especially in designs employing high gain and low seed energy. In this case, OPCPA is particularly susceptible to parasitic depletion of the pump by superfluorescence (SF), the amplification of spontaneous parametric generation at signal and idler wavelengths. In OPCPA, noise gain generally exceeds signal gain during amplification, a result of locally imperfect phase matching of the seed (and/or lack of a seed altogether) throughout the spatiotemporal interaction cross section defined by the pump wave. In the spatial domain, the conical geometry of phase matching about the pump beam gives rise to preferential noise amplification in poorly seeded high-order spatial modes about the signal beam. In the temporal domain, the frequency sweep of the seed pulse results in a higher gain for phase-matched noise available at delays where the seed wavelength is imperfectly phase matched. Large drops in signal-to-noise ratio (SNR) occur especially during amplifier saturation, when there is preferential amplification of coordinates where both signal phase matching and seeding is poorest, thus boosting conversion efficiency and bandwidth but also preferentially amplifying noise. As a result, when gain is high and the initial SNR is low, SF energy can become comparable with or even overtake the amplified signal energy, thus placing a ceiling on the usable energy extractable by the signal and heavily degrading the noise performance.

For example, the half-octave phase-matching bandwidth and 30 ps pump pulse duration of the pioneering $2.1 \,\mu\text{m}$ few-cycle OPCPA system of [9] set the equivalent noise energy of vacuum fluctuations (with the equivalent of one photon per mode [12]) in that amplifier to ~ 40 aJ (4×10^{-17} J). With a 4 pJ seed energy (by DFG of a 5 nJ Ti:S oscillator pulse), the initial SNR was only $\sim 10^5$. After amplification, owing to SF buildup, 80 µJ was the practical limit in amplified signal energy [9], and the full available pump energy could not be employed. Using a Ti:S regenerative amplifier/nonlinear pulse compressor front end to boost the seed energy to a few nanojoules, [10] recently reported 2.1 μ m, 15 fs pulses with 920 μ J of energy in the signal band. This work obtained both good efficiency and excellent bandwidth in the final amplification stage (indicating amplifier saturation)

but with a SF noise level of 20%, resulting in 9% rms energy fluctuations. Despite the increase in seed energy, scaling to higher pulse energies seems difficult.

This Letter outlines techniques essential for building highly stable, ultrabroadband, high-gain OPCPA systems, demonstrated here in a 2.2 μ m system with energy stability comparable to the standard of commercial high-peak-power Ti:S laser systems (1.5% rms energy and 0.8% rms intensity fluctuations). We obtain a clean amplified signal spectrum and fully compressible pulses while maintaining good efficiency and bandwidth by means of saturation in the final amplification stage. With higher-energy pump pulses, these SF suppression methods should allow scaling of the system to multimillijoule signal energy and potentially terawatt peak powers with noise performance suitable for HHG.

The OPCPA system (see Fig. 1) is constructed as follows. The full power (150 mW) of the 80 MHz Ti:S oscillator is used to generate a passively CEPstabilized, half-octave bandwidth, 2 µm, 3 pJ energy pulse train by intrapulse DFG (mixing of the 650 and 940 nm components) in a 2 mm MgO-doped periodically poled congruent lithium niobate (MgO:PPCLN) crystal (poling period Λ is 13.1 μ m). The spectrum [Fig. 2(a), red dotted curve], covers 1570 to 2470 nm at -20 dB. Once the remaining 1 μ m Ti:S light is sent to the pump amplifier chain, the $2 \mu m$ seed pulses are stretched using normal dispersion in a 30 mm block of bulk silicon to 6.2 ps length (full width at -10 dB) and then preamplified in an optical parameter amplifier (OPA), OPA1 (3 mm MgO:PP-CLN, $\Lambda = 31.0 \ \mu \text{m}$), to 1.5 μJ . After OPA1, an acoustooptic programmable dispersive filter (AOPDF, Fastlite) increases the signal duration to 9.5 ps, both optimizing efficiency-bandwidth product and SF suppression in the power amplifier stage [13] and compensating for higher-order dispersion mismatch between the stretcher and compressor materials. Losses from the AOPDF ($\sim 90\%$) and spatial filters are compensated by OPA2. The resulting 5 μ J pulse is amplified to 220 μ J in OPA3 and compressed in three passes through an antireflection-coated 10 cm. high-purity quartz glass block that introduces ~10% loss. The OPA2 and OPA3 crystals are, respectively, 3-mm- and 1.6-mm-length stoichiometric lithium tantalate (MgO:PPSLT) gratings with $\Lambda = 31.4 \mu m$. In all stages, a 1° angle between pump and signal beams allows separation of signal and idler after amplification. Figure 2 shows the amplified spectrum [(a), black, solid] and the corresponding interferometric autocorrelation trace [(b), black, solid] of the final

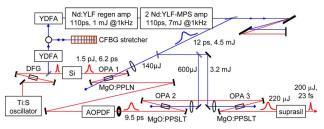


Fig. 1. (Color online) Schematic of the OPCPA system.

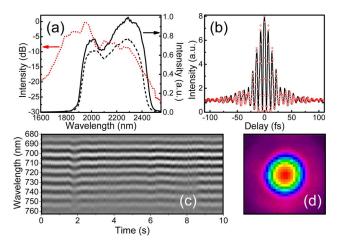


Fig. 2. (Color online) (a) DFG spectrum (red, dotted) and amplified signal spectrum (black; solid and dashed curves are at 220 $\mu\mathrm{J}$ and 170 $\mu\mathrm{J}$ energy, respectively.) (b) Interferometric autocorrelation of the compressed 220 $\mu\mathrm{J}$ pulse by second-harmonic generation in β -barium borate (solid) and the transform limit (circles) calculated from the spectrum in (a). (c) f-3f interferogram, indicating 150 mrad rms CEP fluctuations over 10 s. (d) Pseudocolor pyrolelectric CCD image of the 2 $\mu\mathrm{m}$ output beam.

 $2.2~\mu m$ pulse. It is compressed to 23 fs (1.1× its transform limit), or three cycles, FWHM.

The 4.5 W pump laser system produces 4.5 mJ, 12 ps. 1 µm pulses. It consists sequentially of two Ybdoped fiber amplifiers (YDFA), an Nd:YLF regenerative amplifier, and two Nd:YLF multipass slab (MPS) amplifiers and is seeded by the 1047 nm component of the Ti:S oscillator. To reduce the peak power in the MPS amplifiers, a chirped fiber Bragg grating (CFBG) is placed between YDFA stages and imparts 440 ps/nm group delay, resulting in a 1 kHz, 110 ps, 1.05 mJ pulse train with 0.25 nm bandwidth from the regenerative amplifier (High-Q Laser). The two three-pass MPS amplifiers (Q-Peak MPS gain modules) are customized to avoid B-integral-related damage. Each module is 28 mm long, 2 mm by 6 mm in aperture, and side pumped with 78 W optical power. Employing gains of 2.9 and 2.4, respectively, we obtain 7 mJ pulses. After compression in a grating pair, we obtain 4.5 mJ, 12 ps Gaussian pulses (at FWHM, $\sim 1.3 \times$ their transform limit).

Methods for SF noise suppression are summarized as follows. First, the stretcher/compressor scheme maximizes the 2 μ m seed energy by avoiding lossy elements in the pulse stretcher. In comparison to [9,10], we use an AOPDF as a compensator for stretcher/compressor dispersion mismatch rather than as a stretcher, placing it between pre- and power amplifier stages where its 90% transmission losses do not affect the seed energy of OPA1 and can be compensated by OPA2. This increases the initial SNR by 1 order of magnitude.

Second, we use multiple apertures after OPA1 to eliminate the phase-matched, SF-dominated high-order spatial modes of the signal. In addition to a hard aperture after OPA1, by setting the pump beam width less than half the signal beam width in OPA2 and OPA3 and placing the nonlinear crystal 2–3 dif-

fraction lengths away from the signal focus, the amplifiers act as soft apertures and spatial filters. The apertures clean the signal beam by sequentially selecting a smaller portion of the initial seed beam. This cleans the wavefront, preserves only the region of the beam with highest SNR, eliminates a slight spatial chirp from the AOPDF, and impresses the clean pump beam profile on the amplified signal. AOPDF and aperture losses are recovered in OPA2. This ensures the final amplification stage (OPA3) gain is kept as low as possible in order to maximize the conversion efficiency.

Third, we carefully optimize the signal duration and spectrum at each stage. Here, several features of SF growth in OPCPA are relevant [13]; each temporal coordinate is essentially an independent amplifier, with local signal frequency and SNR; SF gain equals signal gain when the signal is perfectly phase matched but is otherwise greater, with the discrepancy increasing with the local signal phase mismatch, and unseeded temporal coordinates close to the pump pulse peak are most susceptible to depletion of the pump by SF. Optimization of SF suppression in ultrabroadband OPCPA requires, therefore, that all signal frequencies near the pump pulse peak are well seeded, and the signal is chirped enough to push frequencies at the edge of the phase-matching bandwidth away from the pump pulse peak. This results in a slight sacrifice in amplifier bandwidth relative to the full phase-matching bandwidth but strongly improves SF suppression. Separate optimization of seed chirp at each stage is necessary, since the peak gain determines the duration of the OPA gain window (i.e., the degree of temporal gain narrowing). To ensure these conditions, we use a broadband seed with a spectrum spanning $1.6-2.5 \mu m$, covering the full phase-matching bandwidth, but, through adequate chirp, limit the effective amplifier bandwidth at each stage to a central 600-nm-wide wavelength range. Seed chirps corresponding to signal durations of 6.2 and 9.5 ps for OPA1 (10⁶ gain) and OPA2 /OPA3 (10²-10³ gain), achieve this.

Finally, while some amplifier saturation in the final stage is necessary to obtain good conversion efficiency and is helpful in suppressing gain fluctuations due to pump intensity noise, in all stages we avoid pushing hard into saturation (as a tool to expand the effective amplifier bandwidth), since this preferentially amplifies coordinates of the signal pulse where the difference between SF and signal gain is highest.

As a result of these methods, we obtain a clean signal spectrum (single shot), 1.5% rms energy fluctuation of the 220 μ J amplified pulse, and 0.8% rms peak intensity fluctuation after compression, while maintaining a conversion efficiency of 7% (comparable to [10]) and enough bandwidth to support a three-cycle pulse. These numbers (and a 15% rms SF energy fluctuation measured in the absence of a seed pulse) allow us to calculate an SF level of 7%. With slightly less saturation in OPA3, we can obtain 170 μ J with slightly narrower spectrum (Fig. 2, dashed curve) and 2% SF. Using higher-energy pump pulses at OPA2 and OPA3, we estimate we will be

able to further amplify the signal to the millijoule level while maintaining suppression of SF to $<\!10\%$ of the total energy without the need for costly high-energy seed generation. The CEP fluctuation, measured by an f-to-3f spectral interferometer, is 150 mrad rms over 10 s [Fig. 2(c)], where the residual phase excursion at time= $\sim\!2$ s was traceable to amplitude-to-phase noise coupling in the continuum generation arm of the interferometer. No significant CEP drift is observed over 10 s. Finally, excellent beam and wavefront quality (M^2 =1.3) allows high-quality focusing. With 200 $\mu\rm J$ and a $\sim\!50~\mu\rm m$ waist, our beam generates a 2-mm-long plasma column in air.

In conclusion, we have demonstrated techniques of general use for highly stable ultrabroadband OPCPA with excellent noise performance even while maintaining high conversion efficiency and bandwidth in the final stage. Energy scaling of the demonstrated OPCPA system may provide a route toward the development of high-flux extreme UV and soft-x-ray HHG sources.

This work was financially supported by the U.S. Defense Advanced Research Project Agency (DARPA) Hyperspectral Source program via U.S. Air Force Office of Scientific Research (AFOSR) grants FA9550-06-1-0468 and FA9550-07-1-0014 and the Australian Research Council Centre of Excellence program.

References

- M. Lewenstein, Ph. Balcou, M. Yu. Ivanov, A. L'Huillier, and P. B. Corkum, Phys. Rev. A 49, 2117 (1994).
- B. Shan and Z. H. Chang, Phys. Rev. A 65, 011804 (2002).
- A. Gordon and F. Kärtner, Opt. Express 13, 2941 (2005).
- K. D. Schultz, C. I. Blaga, R. Chirla, P. Colosimo, J. Cryan, A. M. March, C. Roedig, E. Sistrunk, J. Tate, J. Wheeler, P. Agostini, and L. F. Dimauro, J. Mod. Opt. 54, 1075 (2007).
- 5. V. S. Yakovlev, M. Ivanov, and F. Krausz, Opt. Express **15**, 15351 (2007).
- T. Popmintchev, M.-C. Chen, O. Cohen, M. E. Grisham, J. J. Rocca, M. M. Murnane, and H. C. Kapteyn, Opt. Lett. 33, 2128 (2008).
- S. Witte, R. Th. Zinkstok, A. L. Wolf, W. Hogervorst, W. Ubachs, and K. S. E. Eikema, Opt. Express 14, 8168 (2006)
- F. Tavella, A. Marcinkevičius, and F. Krausz, Opt. Express 14, 12822 (2006).
- T. Fuji, N. Ishii, C. Y. Teisset, X. Gu, T. Metzger, A. Baltuška, N. Forget, D. Kaplan, A. Galvanauskas, and F. Krausz, Opt. Lett. 31, 1103 (2006).
- 10. X. Gu, G. Marcus, Y. Deng, T. Metzger, C. Teisset, N. Ishii, T. Fuji, A. Baltuška, R. Butkus, V. Pervak, H. Ishizuki, T. Taira, T. Kobayashi, R. Kienberger, and F. Krausz, Opt. Express 17, 62 (2009).
- K.-H. Hong, A. Siddiqui, J. Moses, J. Gopinath, J. Hybl, F. Ö. Ilday, T. Y. Fan, and F. X. Kärtner, Opt. Lett. 33, 2473 (2008).
- 12. H. A. Haus, *Electromagnetic Noise and Quantum Optical Measurements* (Springer-Verlag, 2000).
- J. Moses, C. Manzoni, S.-W. Huang, G. Cerullo, and F. X. Kärtner, Opt. Express 17, 5540 (2009).